A lysosome-to-nucleus signalling mechanism senses and regulates the lysosome via mTOR and TFEB

Citation: Settembre, Carmine, Roberto Zoncu, Diego L Medina, Francesco Vetrini, Serkan Erdin, SerpilUckac Erdin, Tuong Huynh, et al. "A Lysosome-to-Nucleus Signalling Mechanism Senses and Regulates the Lysosome via mTOR and TFEB." The EMBO Journal 31, no. 5 (February 17, 2012): 1095–1108.

As Published: http://dx.doi.org/10.1038/emboj.2012.32

Publisher: EMBRO Press

Persistent URL: http://hdl.handle.net/1721.1/96733

Version: Final published version: final published article, as it appeared in a journal, conference proceedings, or other formally published context

The EMBO Journal (2012) 31, 1095–1108 | © 2012 European Molecular Biology Organization | Some Rights Reserved 0261-4189/12
www.embojournal.org

THE EMBO JOURNAL

EMBO open

A lysosome-to-nucleus signalling mechanism senses and regulates the lysosome via mTOR and TFEB

Since Advance Online Publication, the penultimate author name has been corrected.

Carmine Settembre[1,2,3,13], Roberto Zoncu[4,5,6,13], Diego L Medina[1], Francesco Vetrini[1,2,3], Serkan Erdin[2], SerpilUckac Erdin[2,3], Tuong Huynh[2,3], Mathieu Ferron[7], Gerard Karsenty[7], Michel C Vellard[8], Valeria Facchinetti[9], David M Sabatini[4,5,6,10,11] and Andrea Ballabio[1,2,3,12,*]

[1]Telethon Institute of Genetics and Medicine (TIGEM), Naples, Italy, [2]Department of Molecular and Human Genetics, Baylor College of Medicine, Houston, TX, USA, [3]Jan and Dan Duncan Neurological Research Institute, Texas Children's Hospital, Houston, TX, USA, [4]Whitehead Institute for Biomedical Research, Nine Cambridge Center, Cambridge, MA, USA, [5]Department of Biology, Massachusetts Institute of Technology (MIT), Cambridge, MA, USA, [6]David H Koch Institute for Integrative Cancer Research at MIT, Cambridge, MA, USA, [7]Department of Genetics and Development, College of Physicians and Surgeons, Columbia University, New York, NY, USA, [8]BioMarin Pharmaceutical Inc, Novato, CA, USA, [9]Department of Immunology, Center for Cancer Immunology Research, The University of Texas MD Anderson Cancer Center, Houston, TX, USA, [10]Seven Cambridge Center, Broad Institute, Cambridge, MA, USA, [11]Howard Hughes Medical Institute, MIT, Cambridge, MA, USA and [12]Medical Genetics, Department of Pediatrics, Federico II University, Naples, Italy

The lysosome plays a key role in cellular homeostasis by controlling both cellular clearance and energy production to respond to environmental cues. However, the mechanisms mediating lysosomal adaptation are largely unknown. Here, we show that the Transcription Factor EB (TFEB), a master regulator of lysosomal biogenesis, colocalizes with master growth regulator mTOR complex 1 (mTORC1) on the lysosomal membrane. When nutrients are present, phosphorylation of TFEB by mTORC1 inhibits TFEB activity. Conversely, pharmacological inhibition of mTORC1, as well as starvation and lysosomal disruption, activates TFEB by promoting its nuclear translocation. In addition, the transcriptional response of lysosomal and autophagic genes to either lysosomal dysfunction or pharmacological inhibition of mTORC1 is suppressed in TFEB−/− cells. Interestingly, the Rag GTPase complex, which senses lysosomal amino acids and activates mTORC1, is both necessary and sufficient to regulate starvation- and stress-induced nuclear translocation of TFEB. These data indicate that the lysosome senses its content and regulates its own biogenesis by a lysosome-to-nucleus signalling mechanism that involves TFEB and mTOR.

*Corresponding author. Telethon Institute of Genetics and Medicine (TIGEM), Via Pietro Castellino 111, Naples 80131, Italy.
Tel.: +39 081 6132207; Fax: +39 081 579 0919;
E-mail: ballabio@tigem.it
[13]These authors contributed equally to this work

Received: 22 December 2011; accepted: 27 January 2012; published online: 17 February 2012; corrected: 7 March 2012

The EMBO Journal (2012) **31,** 1095–1108. doi:10.1038/emboj.2012.32; Published online 17 February 2012
Subject Categories: membranes & transport; signal transduction
Keywords: autophagy; cellular clearance; endocytosis; starvation

Introduction

The lysosome maintains cellular homeostasis and mediates a variety of physiological processes, including cellular clearance, lipid homeostasis, energy metabolism, plasma membrane repair, bone remodelling, and pathogen defense. All these processes require an adaptive and dynamic response of the lysosome to environmental cues. Indeed, physiologic cues, such as ageing and diet, and pathologic conditions, which include lysosomal storage diseases (LSDs), neurodegenerative diseases, injuries, and infections may generate an adaptive response of the lysosome (Luzio *et al*, 2007; Ballabio and Gieselmann, 2009; Saftig and Klumperman, 2009).

Our understanding of the mechanisms that regulate lysosomal function and underlying lysosomal adaptation is still in an initial phase. A major player in the regulation of lysosomal biogenesis is the basic Helix-Loop-Helix (bHLH) leucine zipper transcription factor, TFEB (Sardiello *et al*, 2009). Among the identified TFEB transcriptional targets are lysosomal hydrolases that are involved in substrate degradation, lysosomal membrane proteins that mediate the interaction of the lysosome with other cellular structures, and components of the vacuolar H^+-ATPase (v-ATPase) complex that participate in lysosomal acidification (Sardiello *et al*, 2009; Palmieri *et al*, 2011). TFEB is also a main player in the transcriptional response to starvation and controls autophagy by positively regulating autophagosome formation and autophagosome–lysosome fusion both *in vitro* and *in vivo* (Settembre *et al*, 2011). TFEB activity and its nuclear translocation correlate with its phosphorylation status (Settembre and Ballabio, 2011; Settembre *et al*, 2011). However, it is still unclear how the cell regulates TFEB activity according to its needs.

An intriguing hypothesis is that the lysosome senses the physiological and nutritional status of the cell and conveys this information to the nucleus to drive the activation of feedback gene expression programs. A 'sensing device', which is responsive to the lysosomal amino acid content and involves both the v-ATPase and the master growth regulator mTOR complex 1 (mTORC1), was recently identified on the lysosomal surface (Zoncu *et al*, 2011a). The interaction between amino acids and v-ATPase regulates Rag guanosine triphosphatases (GTPases), which in turn activate mTORC1 by translocating it to the lysosomal surface (Sancak *et al*, 2008, 2010; Zoncu *et al*, 2011a). According to this mechanism, the lysosome participates in the signalling

pathways regulated by mTOR, which controls several cellular biosynthetic and catabolic processes (Zoncu *et al*, 2011b).

We postulated that TFEB uses the v-ATPase/mTORC1 sensing device on the lysosomal surface to modulate lysosomal function according to cellular needs. Consistent with this hypothesis, we found that TFEB interacts with mTOR on the lysosomal membrane and, through this interaction, it senses the lysosomal content. Therefore, TFEB acts both as a sensor of lysosomal state, when on the lysosomal surface, and as an effector of lysosomal function when in the nucleus. This unique lysosome-to-nucleus signalling mechanism allows the lysosome to regulate its own function.

Results

TFEB responds to the lysosomal status

We postulated that TFEB activity was regulated by the physiological status of the lysosome. Therefore, we tested whether disruption of lysosomal function had an impact on TFEB nuclear translocation. TFEB subcellular localization was analysed in HeLa and HEK-293T cells transiently transfected with a TFEB–3 × FLAG plasmid and treated overnight with several inhibitors of lysosomal function. These treatments included the use of chloroquine (CQ), an inhibitor of the lysosomal pH gradient, and Salicylihalamide A (SalA), a selective inhibitor of the v-ATPase (Xie *et al*, 2004), as well as overexpression of PAT1, an amino acid transporter that causes massive transport of amino acids out of the lysosomal lumen (Sagne *et al*, 2001). Immunofluorescence analysis showed a striking nuclear accumulation of TFEB–3 × FLAG in treated cells (Figure 1A and B). We repeated this analysis using an antibody detecting the endogenous TFEB (Supplementary Figure S1). Similarly to their effect on exogenously expressed TFEB, both amino acid starvation and lysosomal stress induced nuclear translocation of endogenous TFEB (Figure 1C). These observations were confirmed by immunoblotting performed after nuclear/cytoplasmic fractionation (Figure 1D). Immunoblotting also revealed that TFEB nuclear accumulation was associated with a shift of TFEB–3 × FLAG to a lower molecular weight, suggesting that lysosomal stress may affect TFEB phosphorylation status (Figure 1D).

mTORC1 regulates TFEB subcellular localization

Based on the observation that mTORC1 resides on the lysosomal membrane and its activity is dependent on both nutrients and lysosomal function (Sancak *et al*, 2010; Zoncu *et al*, 2011a), we postulated that the effects of lysosomal stress on TFEB nuclear translocation may be mediated by mTORC1. Consistent with this idea, chloroquine or SalA inhibited mTORC1 activity as measured by level of p-P70S6K, a known mTORC1 substrate (Figure 2A; Zoncu *et al*, 2011a). The involvement of mTOR appears in contrast with our previous observation that Rapamycin, a known mTOR inhibitor, did not affect TFEB activity. However, recent data indicate that Rapamycin is a partial inhibitor of mTOR, as some substrates are still efficiently phosphorylated in the presence of this drug (Thoreen *et al*, 2009). Therefore, we used kinase inhibitors Torin 1 and Torin2, which belong to a novel class of molecules that target the mTOR catalytic site, thereby completely inhibiting mTOR activity (Feldman *et al*, 2009; Garcia-Martinez *et al*, 2009; Thoreen *et al*, 2009).

We stimulated starved cells, in which TFEB is dephosphorylated and localized to the nucleus, with an amino acid rich medium supplemented with Torin 1 (250 nM), Rapamycin (2.5 μM), or ERK inhibitor U0126 (50 μM). Stimulation of starved cells with nutrients alone induced a significant TFEB molecular weight shift and re-localization to the cytoplasm (Figure 2B). Nutrient stimulation in the presence of the ERK inhibitor U0126 at a concentration of 50 μm induced only a partial TFEB molecular weight shift, suggesting that phosphorylation by ERK partially contributes to TFEB cytoplasmic localization. Treatment with 2.5 μM Rapamycin also resulted in a partial molecular weight shift but did not affect TFEB subcellular localization (Figure 2B), consistent with our previous observations (Settembre *et al*, 2011). However, Torin 1 (250 nM) treatment entirely prevented the molecular weight shift induced by nutrients and, in turn, resulted in massive TFEB nuclear accumulation. This conclusion is in contrast with a recent study that showed that mTOR-mediated TFEB phosphorylation promoted, rather than inhibited, its nuclear translocation (Pena-Llopis *et al*, 2011). Instead our data indicate that mTOR is a potent inhibitor of TFEB nuclear translocation and that TFEB is a rapamycin-resistant substrate of mTORC1.

In a previous study, we showed that ERK2 phosphorylates TFEB and that starvation and ERK2 inhibition promote TFEB nuclear translocation (Settembre *et al*, 2011). We tested whether lysosomal stress caused TFEB nuclear translocation also via ERK inhibition. Overnight treatment of HeLa cells with either chloroquine or SalA did not have any effect on ERK activity (Figure 2A), suggesting that mTOR-mediated regulation is predominant. To quantify the effects of ERK and mTOR on TFEB subcellular localization, we developed a cell-based high content assay using stable HeLa cells that overexpress TFEB fused to the green fluorescent protein (TFEB–GFP) (see Materials and methods for details). We tested 10 different concentrations of each inhibitor (U0126, Rapamycin, Torin 1, and Torin 2) ranging from 2.54 nM to 50 μM. Figure 2C and D shows the TFEB nuclear/cytoplasmic distribution for each concentration of each compound in duplicate represented as dose–response curves using a non-linear regression fitting (see Materials and methods for details). Consistent with the above-described data, the most potent compounds that activate TFEB nuclear translocation were Torin 1 (EC50; 147.9 nM) and its analogue Torin 2 (EC50; 1666 nM). ERK inhibitor U0126 showed only a partial effect, while Rapamycin had no effects at any of the concentrations that are routinely used (10 nM–10 μM). Furthermore, Torin 1 treatment potently induced nuclear accumulation of endogenous TFEB in HEK-293T cells (Figure 2E), confirming the observations obtained with the TFEB–GFP construct.

As Torin 1 inhibits both mTORC1 and mTORC2 complexes, we next evaluated the contribution of each complex to TFEB regulation. Three main observations suggest that TFEB is predominantly regulated by mTORC1: (1) stimulation of starved cells with amino acids, which activate mTORC1 but not mTORC2, induced an extensive TFEB molecular weight shift, which is highly suggestive of a phosphorylation event (Supplementary Figure S2); (2) knockdown of RagC and RagD, which mediate amino acid signals to mTORC1, caused TFEB nuclear accumulation even in cells kept in full nutrient medium (Figure 2F); (3) in cells with disrupted mTORC2 signalling (Sin1−/− mouse embryonic fibroblasts (MEFs)) (Frias *et al*, 2006; Jacinto *et al*, 2006; Yang *et al*, 2006) TFEB

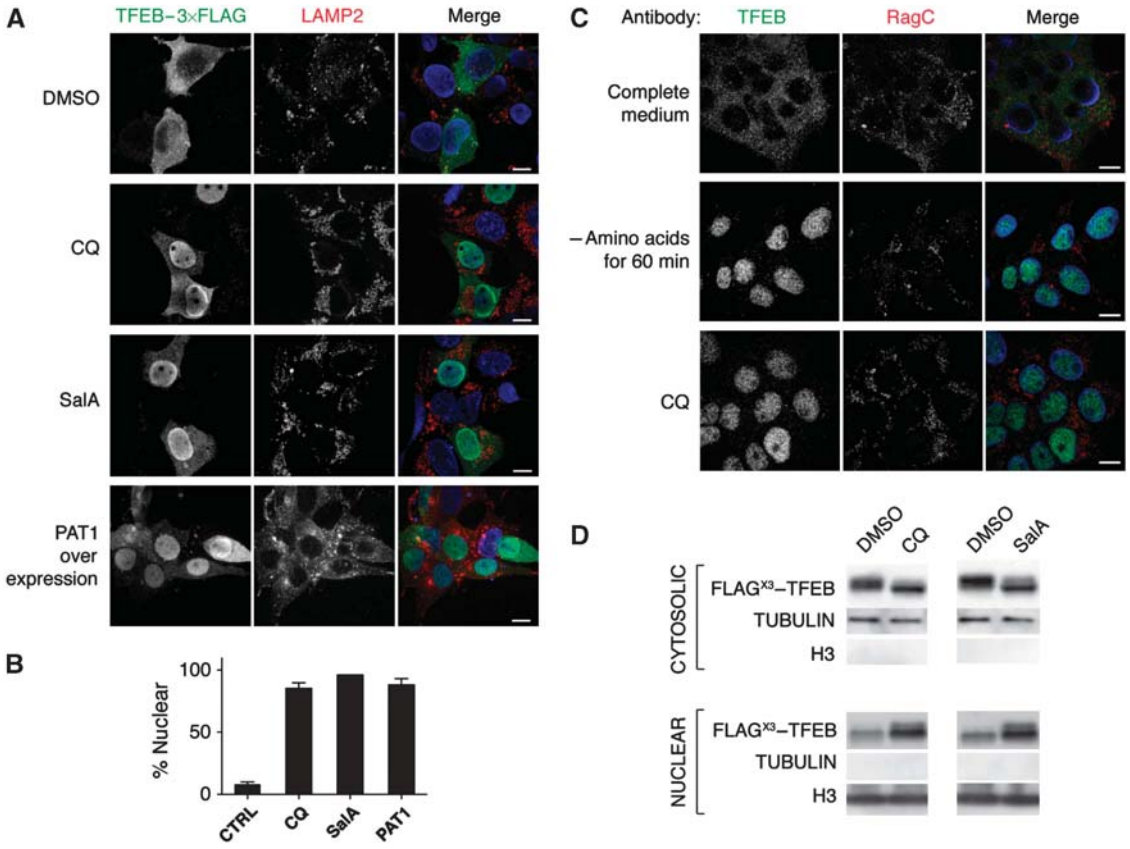

Figure 1 Lysosomal stress induces TFEB nuclear translocation. (**A**) Immunofluorescence of HEK-293T cells that express TFEB–3 × FLAG, subjected to the indicated treatments and stained with antibodies against FLAG and the lysosomal marker LAMP2. The FLAG and LAMP2 channels are in green and red, respectively, in the merge. DAPI (blue) is included in the merge. Scale bars represent 10 μm. (**B**) Quantification of the number of cells with nuclear TFEB–3 × FLAG in the four conditions in (**A**). Each value represents mean ± s.d. from three independent fields with $N = 300$. (**C**) Immunofluorescence of HEK-293T cells treated as indicated and stained with antibodies against endogenous TFEB and the lysosomal protein RagC (green and red, respectively, in the merge). DAPI is included in the merge. Scale bars represent 10 μm. (**D**) Immunoblotting of proteins extracted from HeLa cells that express TFEB–3 × FLAG treated with DMSO, chloroquine (CQ) or SalA, subjected to nuclear/cytosolic fractionation and blotted with antibody against FLAG to detect TFEB. H3 and tubulin were used as nuclear and cytosolic markers, respectively. Blots are representative of triplicate experiments.

underwent a molecular weight shift and nuclear translocation upon Torin 1 treatment that were similar to control cells (Figure 2G). Together, these data indicate that mTORC1, not mTORC2, regulates TFEB by preventing its nuclear translocation. Finally, co-immunoprecipitation assays in HEK-293T cells expressing TFEB–3 × FLAG showed that TFEB binds both to mTOR and to the mTORC1 subunit raptor but not to the mTORC2 subunits rictor and mSin1, indicating that TFEB and mTORC1 interact both functionally and physically (Figure 2H).

mTORC1 controls TFEB subcellular localization via phosphorylation of S142

We previously identified phosphorylation at Serine 142 as a key event for TFEB nuclear translocation during starvation (Settembre *et al*, 2011). To test whether mTORC1 phosphorylates TFEB at S142, we generated a phosphospecific antibody that recognizes TFEB only when phosphorylated at S142. No signal was detected by this antibody in cells that overexpress the S142A mutant version of TFEB, thus confirming its specificity (Supplementary Figure S3). Using this antibody, we observed that TFEB was no longer phosphorylated at S142 in HeLa cells stably overexpressing TFEB–3 × FLAG and cultured in nutrient-depleted media, consistent with our previous results (Figure 3A).

Subsequently, we analysed the levels of S142 phosphorylation in starved cells supplemented with normal media with or without either Torin 1 or Rapamycin. While Torin 1 clearly blunted nutrient-induced S142 phosphorylation, rapamycin did not, suggesting that S142 represents a rapamycin-resistant mTORC1 site (Figure 3A). Indeed, an mTOR kinase assay revealed that mTORC1 phosphorylates highly purified TFEB *in vitro* with comparable efficiency to other known mTORC1 substrates, and this phosphorylation dropped dramatically when mTORC1 was incubated with the S142A mutant version of TFEB (Figure 3B). These results clearly demonstrate that TFEB is an mTOR substrate and that S142 is a key residue for the phosphorylation of TFEB by mTOR.

Recent findings suggest that mTORC1 phosphorylates its target proteins at multiple sites (Hsu *et al*, 2011; Peterson *et al*, 2011; Yu *et al*, 2011). To identify additional serine residues that may be phosphorylated by mTOR, we searched for consensus phosphoacceptor motif for mTORC1 (Hsu *et al*, 2011) in the coding sequence of TFEB (Figure 3C and D).

We mutagenized all TFEB amino acid residues that were putative mTORC1 targets into alanines. We then tested the

effects of each of these mutations on TFEB subcellular localization and found that, similarly to S142A, a serine-to-alanine mutation at position 211 (S211A) resulted in a constitutive nuclear localization of TFEB (Figure 3E). Mutants for the other serine residues behaved similarly to wild-type TFEB (Figure 3E; Supplementary Figure S4; Settembre *et al*, 2011). Together, these data indicate that, in addition to S142, S211 also plays a role in controlling TFEB subcellular localization and suggest that S211 represents an additional target site of mTORC1.

mTORC1 and TFEB interact on the lysosomal surface

Based on the observations that TFEB is a substrate for mTORC1 (Figure 3A and B) and that the two proteins physically interact (Figure 2H), we tested whether the interaction of TFEB and mTORC1 occurs on the lysosomal membrane. Careful examination of HeLa cells that express TFEB–GFP showed that, while under normal growth conditions the majority of cells displayed a predominantly cytoplasmic TFEB localization, a subset of cells showed clearly discernible intracellular puncta of TFEB–GFP fluorescence, suggesting a lysosomal localization (Supplementary Figure S5). These observations were confirmed in MEFs that transiently express TFEB–GFP along with the late endosomal/lysosomal marker mRFP–Rab7 (Figure 4A). In a subset of cells, TFEB–GFP clearly colocalized with mRFP–Rab7-positive lysosomes and this association persisted over time as lysosomes trafficked inside the cell (Figure 4A and B; Supplementary Movie S1).

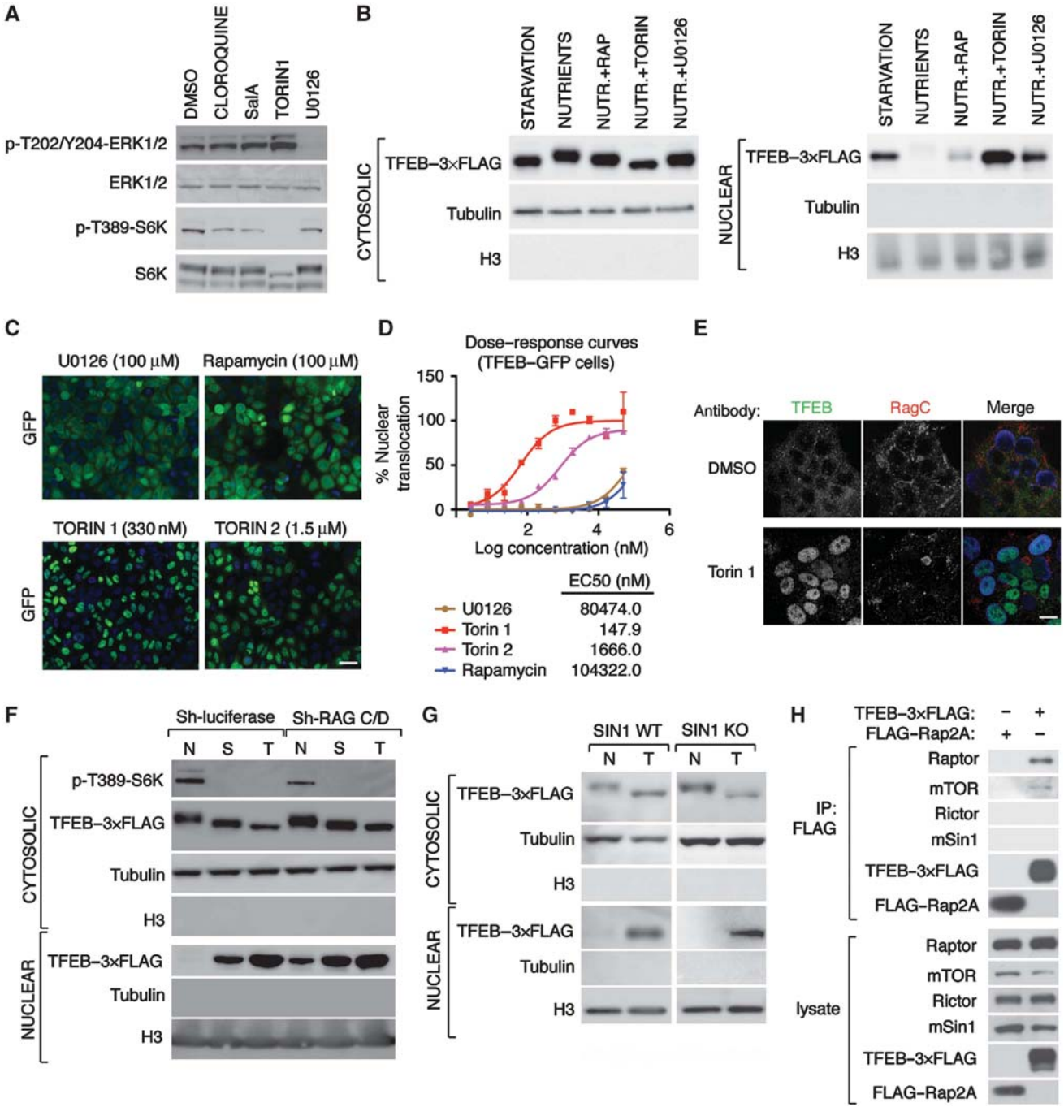

We reasoned that the partial localization of TFEB to lysosomes may be due to a transient binding to mTORC1, followed by mTORC1-dependent phosphorylation and translocation of TFEB to the cytoplasm. To test this idea, we treated TFEB–GFP HeLa cells with Torin 1, as a way to 'trap' TFEB in its bound state to inactive mTORC1. Confirming our hypothesis, Torin 1 caused a massive and dramatic accumulation of TFEB–GFP on lysosomes (Supplementary Figure S5). Similarly, Torin 1 treatment of MEFs resulted in a time-dependent accumulation of TFEB–GFP on lysosomes within minutes of drug delivery, followed by a more gradual accumulation into the nucleus (Figure 4C; Supplementary Movies S2 and S3). Interestingly, we also noticed that Torin 1 treatment caused a significant accumulation of endogenous mTOR on lysosomes compared with untreated cells (Figure 4D). Thus, two mechanisms contribute to clustering of TFEB on lysosomes upon Torin 1 treatment: (1) trapping of the mTORC1–TFEB complex in the inactive state and (2) increase of the amount of mTORC1 bound to the lysosomal surface. The accumulation of inactive mTORC1 on the lysosomal surface may reflect a feedback mechanism through which mTORC1 regulates its own targeting to lysosomal membranes via its kinase activity (Zoncu *et al*, 2011b).

To investigate the lysosomal trapping of TFEB in a dynamic and quantitative way, we performed Fluorescence Recovery After Photobleaching (FRAP) experiments on TFEB–GFP-positive lysosomes (Figure 4E and F; Supplementary Movie S4). In control cells, photobleaching of TFEB–GFP-positive lysosomes was followed by a rapid ($t^{1/2} = 0.35$ min) and substantial (60%) recovery of the initial fluorescence. Conversely, in Torin 1-treated cells, where TFEB–GFP-positive lysosomes were much more prominent and numerous, the fluorescence recovery was slower ($t^{1/2} = 0.57$ min) and smaller (30% recovery of the initial fluorescence). Thus, a large fraction of TFEB was trapped onto the lysosomal surface through binding to inactive mTORC1 and was no longer able to exchange with the cytoplasm.

In conclusion, these data indicate that TFEB and mTORC1 bind to each other on the lysosomal surface, where phosphorylation of TFEB by mTORC1 occurs.

mTORC1 regulates TFEB via the Rag GTPases

The observation that TFEB is regulated by mTORC1 prompted us to determine whether the activation state of the Rag GTPases, which together with the v-ATPase mediate mTORC1 activation by amino acids, played a role in the control of TFEB subcellular localization. Point mutants of the Rags are available, which fully mimic either the presence of amino acids ('$Rags^{CA}$') or their absence ('$Rags^{DN}$') (Sancak *et al*, 2008). We took advantage of these mutants to directly test the requirement for mTORC1 in sequestering TFEB to the lysosome and we asked whether the $Rags^{DN}$ mutants, which cause loss of mTORC1 from the lysosomal surface (Sancak *et al*, 2010), were able to suppress Torin 1-induced lysosomal accumulation of TFEB as well as TFEB-mTORC1 binding. In co-immunoprecipitation assays, Torin 1 clearly boosted the binding of both raptor and mTOR to TFEB–3 × FLAG (Figure 4G). However, co-expression of the $Rags^{DN}$ mutants reduced the binding of TFEB–3 × FLAG to mTORC1 components down to background levels, both in control and in Torin 1-treated cells (Figure 4G). Consistent with these results, immunofluorescence experiments in HEK-293T co-expressing TFEB–3 × FLAG and the $Rags^{DN}$ mutants showed that TFEB failed to cluster on lysosomes following Torin 1 treatment (Figure 4H). Together, these data strongly suggest that TFEB and mTORC1 only interact when they are both found on the lysosomal surface.

Next, we tested whether the activation status of the Rags controlled TFEB nuclear translocation. In HEK-293T cells that co-express TFEB–3 × FLAG and a control small GTPase (Rap2A), amino acid withdrawal caused a massive translocation of TFEB to the nucleus (Figure 5A and D), as previously reported (Settembre *et al*, 2011). Consistent with mTORC1 re-activation, a brief (20 min) re-stimulation of starved cells with amino acids drove TFEB out of the nucleus in the majority of cells (Figure 5A). In contrast, in cells that co-express both TFEB–3 × FLAG and the $Rags^{CA}$ mutants, TFEB localization was always and completely cytoplasmic, regardless of the nutrient state of the cells (Figure 5B and D). Finally, in cells that co-express both TFEB and the $Rags^{DN}$ mutants, TFEB was almost exclusively found in the nucleus and did not translocate to the cytoplasm upon amino acid stimulation (Figure 5C and D). Thus, the activation state of the Rags completely

Figure 2 mTORC1 regulates TFEB. (**A**) Lysosomal stress inhibits mTOR signalling. Immunoblotting of protein extracts isolated from HeLa cells treated overnight as indicated. Membranes were probed with antibodies against p-T202/Y204-ERK1/2, ERK1/2, p-T389-S6K, and S6K to measure ERK and mTORC1 activities. (**B**) Torin 1 induces TFEB dephosphorylation and nuclear translocation. FLAG immunoblotting of cytosolic and nuclear fractions isolated from TFEB–3 × FLAG HeLa cells starved in amino acid-free media and subsequently stimulated as indicated for at least 3 h. Correct subcellular fractionation was verified with H3 and tubulin antibodies. (**C**) Effects of ERK and mTOR inhibitors on TFEB nuclear translocation. TFEB–GFP HeLa cells were seeded in 96-well plates, cultured for 12 h, and then treated with the indicated concentrations of the ERK inhibitor U0126, or the mTOR inhibitors Rapamycin, Torin 1, and Torin 2. After 3 h at 37°C, cells were processed and images were acquired using the OPERA automated confocal microscope (Perkin-Elmer). Scale bars represent 30 μm. (**D**) Dose–response curves of the effects of ERK and mTOR inhibitors on TFEB nuclear translocation. TFEB–GFP HeLa cells were seeded in 384-well plates, cultured for 12 h, and treated with 10 different concentrations of the ERK inhibitor U0126, or the mTOR inhibitors Rapamycin, Torin 1, and Torin 2 ranging from 2.54 nM to 50 μM. The graph shows the percentage of nuclear translocation at the different concentrations of each compound (in log of the concentration). The EC50 for each compound was calculated using Prism software (see Materials and methods for details). (**E**) Immunofluorescence of HEK-293T cells treated with DMSO or Torin 1 and stained with antibodies against endogenous TFEB and the lysosomal protein RagC (green and red, respectively, in the merge). DAPI is included in the merge. Scale bars represent 10 μM. (**F**) Rag GTPase knockdown induces TFEB nuclear translocation. HeLa cells stably expressing TFEB–3 × FLAG were infected with lentiviruses encoding Short hairpin (Sh-) RNAs targeting luciferase (control) or RagC and RagD mRNAs. In all samples, 96 h post infection, cells were left untreated (N = normal media), starved (S = starved media) or treated with Torin 1 (T = Torin 1) for 4 h and then subjected to nuclear/cytosolic fractionation. TFEB localization was detected with a FLAG antibody, whereas tubulin and H3 were used as controls for the cytosolic and nuclear fraction, respectively; levels of S6K phosphorylation were used to test RagC and RagD knockdown efficiency. (**G**) Loss of mTORC2 does not affect TFEB phosphorylation. Mouse embryonic fibroblasts (MEFs) isolated from Sin1−/− or control embryos (E14.5) were infected with a retrovirus encoding TFEB–3 × FLAG; 48 h post infection, cells were treated with Torin 1 (T) for 4 h where indicated, subjected to nuclear/cytosolic fractionation and immunoblotted for FLAG, tubulin, and H3. (**H**) Binding of TFEB to mTORC1. HEK-293T cells that express TFEB–3 × FLAG were lysed and subjected to FLAG immunoprecipitation followed by immunoblotting for mTOR, the mTORC1 subunit raptor and the mTORC2 components rictor and Sin1. FLAG–Rap2A served as negative control.

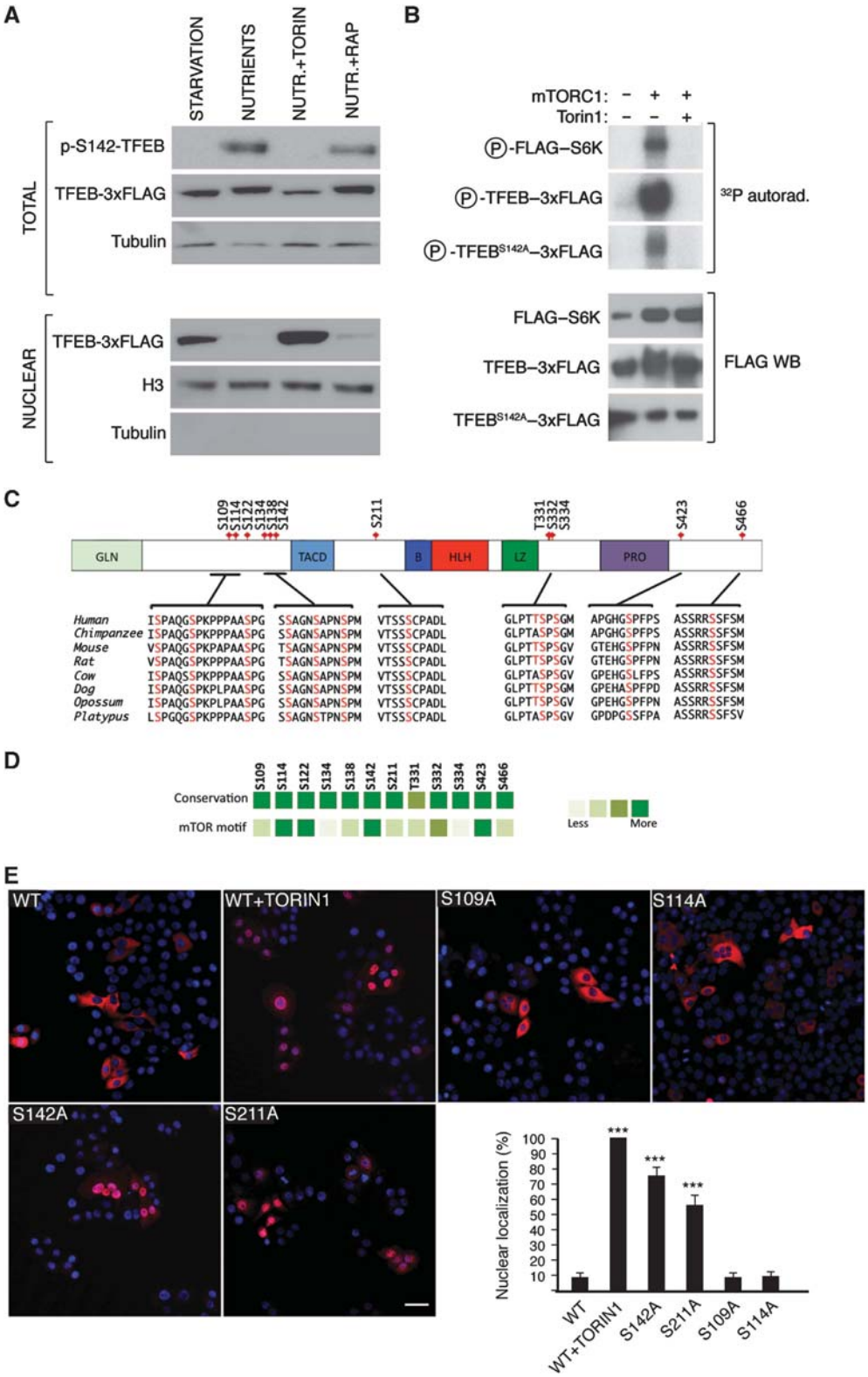

Figure 3 mTORC1 phosphorylates TFEB at serine 142 (S142). (**A**) Torin 1 induces S142 dephosphorylation. HeLa cells were treated as indicated and total and nuclear extracts were probed with a TFEB p-S142 phosphoantibody and with anti-FLAG antibody. Disappearance of TFEB S142 phosphorylation upon starvation or Torin 1 treatment correlates with accumulation of TFEB in the nuclear fraction. (**B**) mTORC1 *in-vitro* kinase assays. Highly purified FLAG–S6K1, TFEB–3 × FLAG, or TFEB^{S142A}–3 × FLAG were incubated with radiolabelled ATP without kinase, with purified mTORC1 or with mTORC1 + Torin 1, and analysed by autoradiography. The lower panel shows a FLAG immunoblot of the substrates. (**C**) Schematic representation of TFEB protein structure with the predicted mTORC1 phosphorylation sites and their conservation among vertebrates (for mTORC1 phophosite prediction see Material and methods). Numbering is according to human isoform 1. (**D**) Sequence conservation scores of the phosphosites and quantitative agreement between mTOR consensus motif and the sequence around the phosphosites of TFEB. (**E**) S142 and S211 regulate TFEB localization. FLAG immunostaining (red) of HeLa cells expressing serine-to-alanine mutated versions of TFEB–3 × FLAG. Nuclei were stained with DAPI (blue). Values are means of five fields containing at least 50 transfected cells. Student's *t*-test (unpaired) $***P<0.001$. Scale bars represent 30 μm.

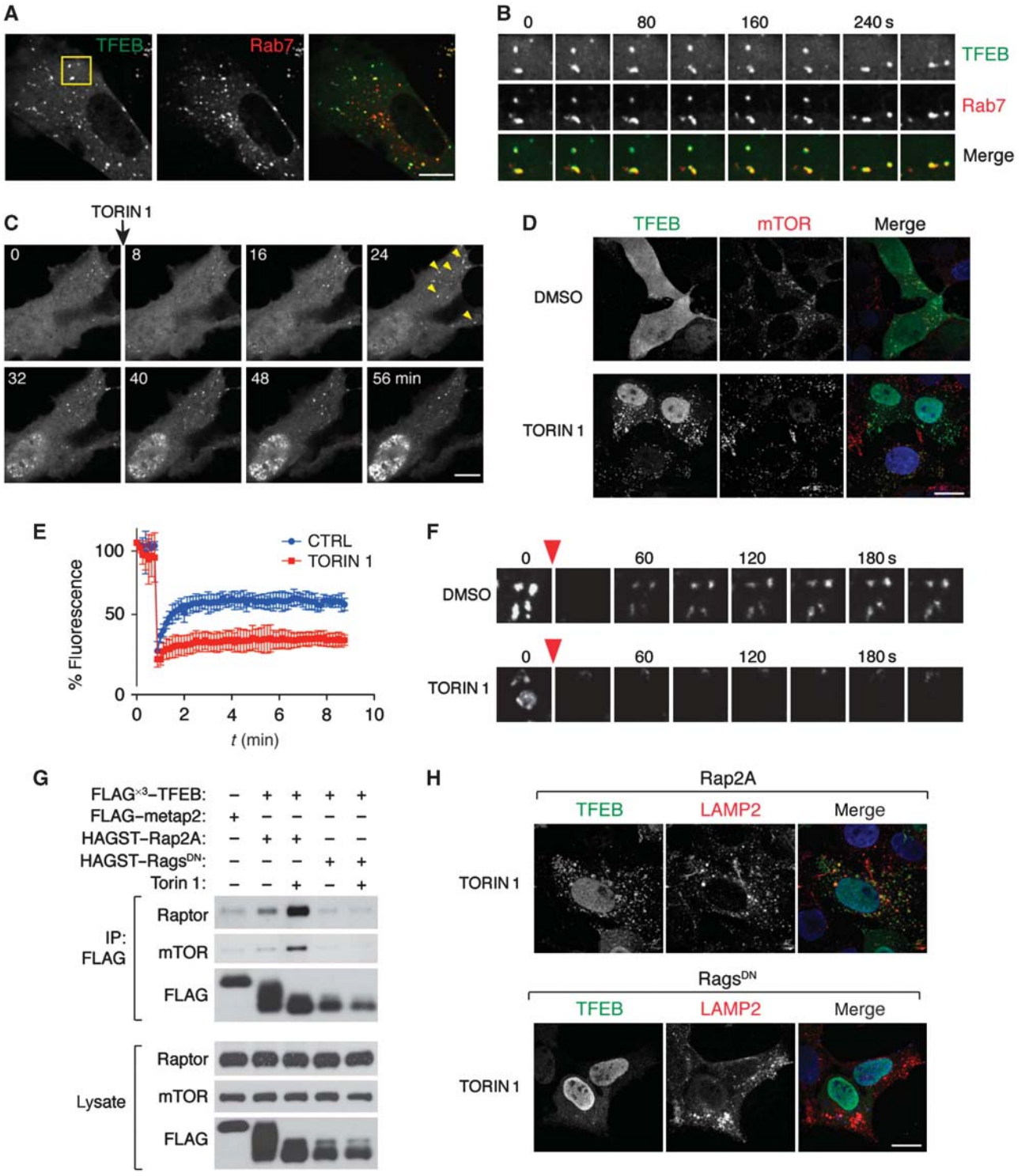

Figure 4 mTORC1 binds and phosphorylates TFEB on the lysosomal surface. (**A**) Spinning disk confocal image of a MEF cell that co-expresses TFEB–GFP and mRFP–Rab7 (green and red in the merge, respectively). (**B**) Time-lapse of TFEB- and Rab7-positive lysosomes from the boxed region in (**A**). Time intervals are in seconds. (**C**) Time-lapse analysis of Torin 1 treatment in a MEF cell expressing TFEB–GFP. Arrow indicates the time of Torin 1 addition. Yellow arrowheads indicate Torin 1-induced lysosomal accumulation of TFEB–GFP. Time intervals are in minutes. (**D**) Immunofluorescence of HEK-293T cells expressing TFEB–3 × FLAG, treated with DMSO (*top*) or Torin1 (*bottom*) and stained with antibodies against FLAG and mTOR (green and red in the merge, respectively; DAPI is in blue). (**E**) FRAP analysis of TFEB–GFP-positive lysosomes from control MEFs (blue) or MEFs treated with Torin 1 (red). Each data point represents mean ± s.d. from five independent spots. (**F**) Time-lapse of photobleaching and fluorescence recovery of TFEB–GFP-positive lysosomes from control-treated MEFs (*top*) or MEFs treated with Torin 1 (*bottom*). Red arrowheads indicate time of photobleaching. Time intervals are in seconds. (**G**) Torin 1 increases binding of TFEB to mTORC1. HEK-293T cells that express TFEB–3 × FLAG along with HAGST-Rap2A or HAGST-Rags^{DN} were treated with vehicle or with Torin1, lysed and subjected to FLAG immunoprecipitation followed by immunoblotting for mTOR and raptor. FLAG–Metap2 served as negative control. (**H**) Immunofluorescence of HEK-293T cells that express TFEB–3 × FLAG along with Rap2A (*top*) or the Rags^{DN} mutants (*bottom*), treated with Torin 1 and stained with antibodies against FLAG and LAMP2 (green and red in the merge, respectively; DAPI is in blue). In all images, scale bars represent 10 μm.

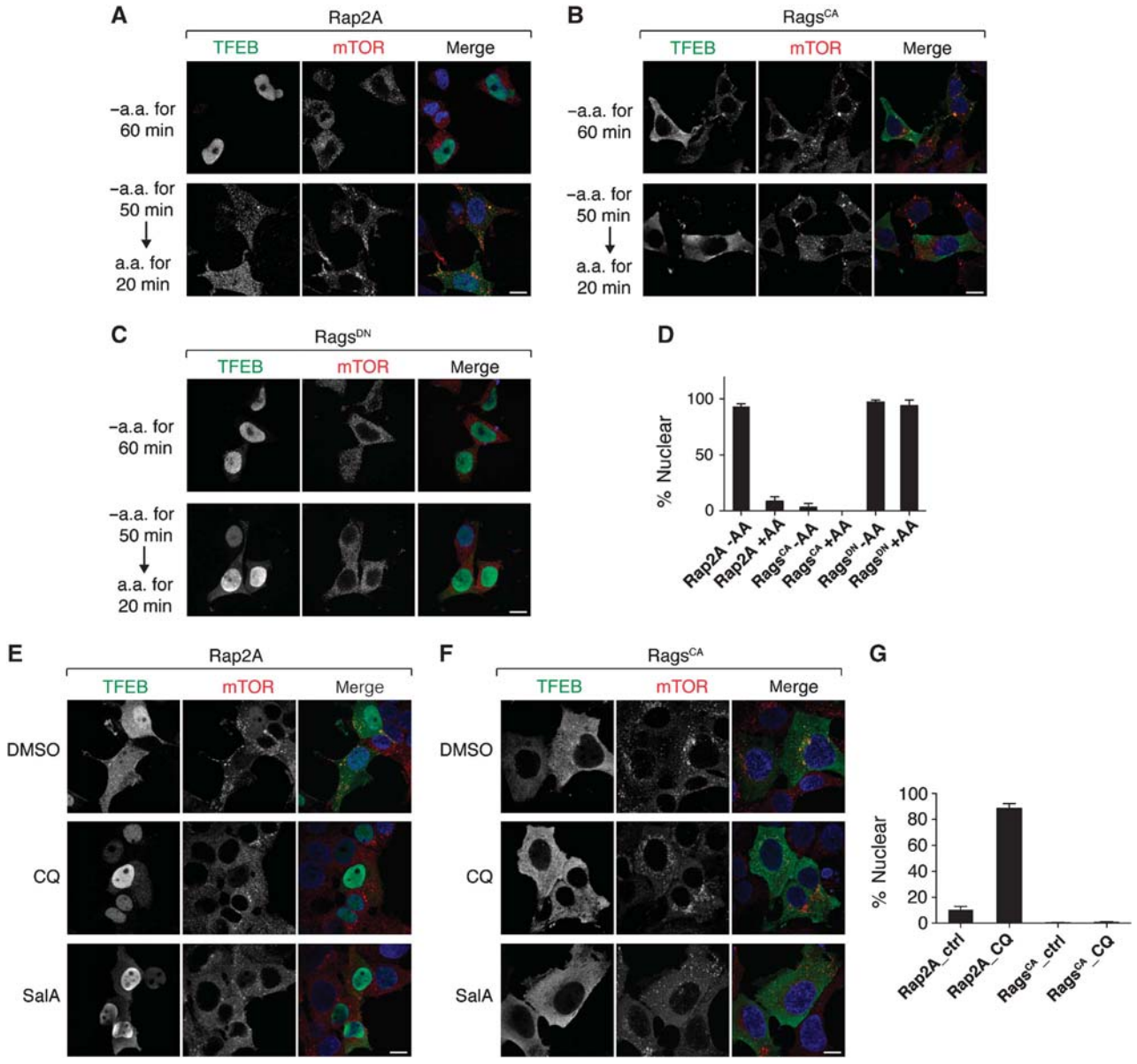

Figure 5 Rag GTPases control TFEB subcellular localization. (**A**–**C**) Immunofluorescence of HEK-293T cells that express TFEB–3 × FLAG along with a control GTPase or the indicated Rag mutants. Cells were deprived of amino acids (*top*) or deprived and then stimulated (*bottom*) for the indicated times and stained for FLAG and mTOR (green and red in the merge, respectively; DAPI is in blue). (**D**) Quantification of the number of cells with nuclear TFEB from each condition in (**A**–**C**). (**E**, **F**) Immunofluorescence of HEK-293T cells that express TFEB–3 × FLAG along with Rap2A (**E**) or the Rags^{CA} mutants (**F**), subjected to the indicated treatments and stained with antibodies against FLAG and mTOR (green and red in the merge, respectively; DAPI is in blue). (**G**) Quantification of the number of cells with nuclear TFEB from DMSO- and CQ-treated fields in (**E**) and (**F**). In all fields, scale bars represent 10 μm. In all histograms, each value represents mean ± s.d. from three independent fields with $N = 300$.

overrides the nutritional status of the cells and is sufficient to determine TFEB localization.

It was previously shown that the Rags^{CA} rescue the inhibitory effect of various lysosomal stressors on mTORC1 activation (Zoncu *et al*, 2011a). Thus, we asked whether the Rags^{CA} mutants were able to prevent the TFEB nuclear translocation promoted by these stressors (Figures 1A–D and 5E). In cells that co-express both TFEB–3 × FLAG and the Rags^{CA} mutants, TFEB remained entirely cytoplasmic upon treatment with Chloroquine and SalA (Figure 5F and G), while it was nuclear in the vast majority of cells that express a control GTPase and were subject to the same drug treatments (Figure 5E and G). Importantly, treatment of cells co-expressing TFEB–GFP and Rag^{CA} with Torin 1 reverted the Rag^{CA}-induced cytoplasmic localization of TFEB and massively drove TFEB to the nucleus, further demonstrating that the action of the Rag mutants on TFEB is mediated by mTORC1 (Supplementary Figure S6).

In summary, these results demonstrate that TFEB localization is directly regulated by the amino acid-mTORC1 signalling pathway via the activation state of Rag GTPases.

The lysosome regulates gene expression via TFEB

As the interaction of TFEB with mTORC1 on the lysosomal membrane controls TFEB nuclear translocation, we tested whether the ability of TFEB to regulate gene expression was also influenced by this interaction. The expression of several

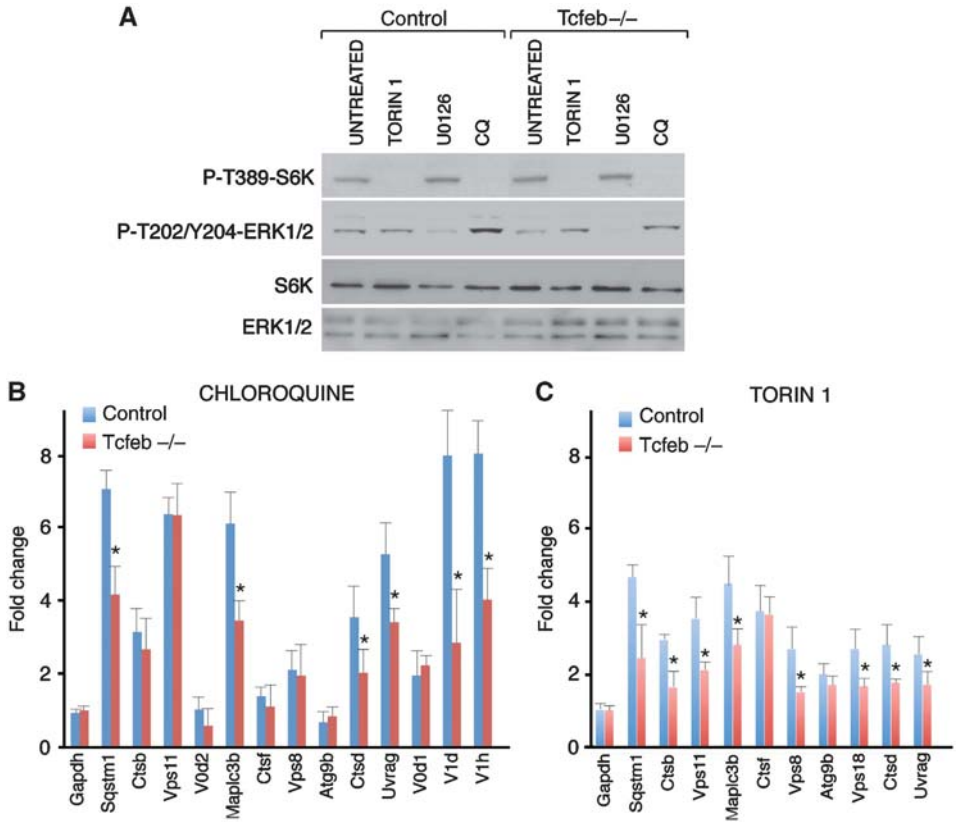

Figure 6 The lysosome regulates gene expression via TFEB. (**A**) Chloroquine treatment inhibits mTORC1 activity in primary hepatocytes. Primary hepatocytes isolated from 2-month-old *Tcfeb*flox/flox (control) and *Tcfeb*flox/flox;Alb-Cre(*Tcfeb*−/−) mice were left untreated, or treated overnight with Torin 1, U0126, or Chloroquine. Subsequently, cells were lysed and protein extracts were immunoblotted with the indicated antibodies. (**B, C**) TFEB mediates the transcriptional response to chloroquine and Torin 1. Quantitative PCR (qPCR) of TFEB target genes in primary hepatocytes from control (flox/flox) and *Tcfeb*−/− mice. Cells were treated with Chloroquine (left) or Torin 1 (right). The graphs show the relative increased expression in the treated versus the corresponding untreated samples. Values represent means ± s.d. of three independent hepatocyte preparations (three mice/genotype). Student's *t*-test (two tailed) **P*-value ⩽0.05.

lysosomal/autophagic genes that were shown to be targets of TFEB (Palmieri *et al*, 2011) was tested in primary hepatocytes from a conditional knockout mouse line in which TFEB was deleted in the liver (*Tcfeb*flox/flox; alb-CRE), and in a control mouse line (*Tcfeb*flox/flox). Cells were treated with either chloroquine or Torin 1, or left untreated. These treatments inhibited mTOR as measured by the level of p-S6K, whereas the levels of p-ERK were unaffected (Figure 6A). Primary hepatocytes isolated from TFEB conditional knockout mice cultured in regular medium did not show significant differences in the expression levels of several TFEB target genes compared with control hepatocytes (Supplementary Figure S7). However, while the expression of TFEB target genes was upregulated in hepatocytes from control mice after treatment with chloroquine, this upregulation was significantly blunted in hepatocytes from TFEB conditional knockout mice (Figure 6B). Similarly, the transcriptional response upon Torin 1 treatment was significantly reduced in hepatocytes from TFEB conditional knockout mice (Figure 6C). Together, these results indicate that TFEB plays a key role in the transcriptional response induced by the lysosome via mTOR.

Discussion

Our study demonstrates that TFEB, a master gene for lysosomal biogenesis, is regulated by the lysosome via the mTOR pathway. mTORC1 and TFEB meet on the lysosomal membrane where mTORC1 phosphorylates TFEB.

We previously reported that ERK2 phosphorylates TFEB and, in cells treated with an MEK inhibitor, the TFEB nuclear fraction was increased (Settembre *et al*, 2011). In the same study, we reported that the mTOR inhibitor rapamycin had little or no effects on TFEB subcellular localization. Here, we compared three different types of kinase inhibitors—MEK inhibitor U0126 and mTOR inhibitors rapamycin, Torin 1, and Torin 2—in their ability to cause a shift in TFEB molecular weight and to induce TFEB nuclear translocation. As shown in Figure 2, Torin 1 and Torin 2 induced TFEB nuclear translocation more efficiently compared to U0126. The more pronounced shift of TFEB molecular weight, which was observed in cells treated with Torin 1, suggests that mTORC1 induces TFEB phosphorylation at multiple sites, either directly or indirectly.

In a recent high throughput mass spectrometry study, TFEB was predicted to be phosphorylated at 11 different residues, thus suggesting a complex regulation of its activity with several phosphorylation sites potentially involved (Dephoure *et al*, 2008). Here, we have used an mTORC1 *in-vitro* kinase assay and a phosphoantibody to demonstrate that serine S142, which we previously found to be phosphorylated by ERK2, is also phosphorylated by mTOR and that this phosphorylation has a crucial role in controlling

TFEB subcellular localization and activity. In addition, we have mutated 12 different serines, which were candidate mTOR phosphorylation sites, into alanines, thus abolishing the corresponding TFEB phosphorylation sites. Testing the effects of each of these mutations on TFEB subcellular localization led to the identification of an additional residue, serine S211, which plays a role in TFEB subcellular localization, confirming the predicted complexity of TFEB regulation by phosphorylation.

Phosphorylation of TFEB by mTOR had already been reported in a previous study (Pena-Llopis *et al*, 2011). However, in that study the authors concluded that mTOR promoted, rather than inhibited, TFEB activity. Several lines of evidence indicate that mTOR inhibits TFEB activity. First, TFEB is entirely nuclear when cells are either starved or treated with Torin1, both conditions in which mTOR activity is profoundly inhibited. Second, treatment of starved cells with nutrients, a condition that boosts mTORC1 activity, resulted in TFEB cytoplasmic accumulation, with TFEB being undetectable in the nuclear fraction. Third, treatment with drugs such as chloroquine or SalA, which inhibit mTORC1 function, induced TFEB nuclear accumulation. Fourth, transfection of mutant Rag proteins that inhibit mTORC1 resulted in nuclear accumulation of TFEB and, conversely, mutant Rags that constitutively activate mTORC1 prevented TFEB nuclear accumulation upon starvation, chloroquine and SalA treatment. Fifth, TFEB is in the nucleus in its low-phosphorylated form, an observation that is consistent with a model in which inhibition, rather than activation, of a kinase induces TFEB nuclear translocation. It is difficult to explain the discrepancy between our observations and those reported by Pena-Llopis *et al*. We considered the possibility that the TSC2-deficient cells that were used in that study may behave differently to other cellular systems in the assays performed. To test this possibility, we analysed TFEB regulation by amino acids, chloroquine and Torin 1 in TSC2−/− cells but obtained the same results that we observed in other cell types both on exogenous TFEB–GFP and on endogenous TFEB (Supplementary Figures S8 and S9, respectively).

Our data indicate that mTORC1 negatively regulates TFEB via the amino acid/Rag GTPase pathway. The phosphorylation status of TFEB and its subcellular localization were entirely determined by the activation state of the Rag GTPases, which regulate mTORC1 activity downstream of amino acids (Kim *et al*, 2008; Sancak *et al*, 2008). In particular, constitutively active Rags rescued nuclear translocation of TFEB caused by starvation and lysosomal stress, while inactive Rag mutants caused TFEB to accumulate in the nucleus even in fully fed cells. These results imply that, among the many regulatory inputs to mTORC1, the amino acid pathway is particularly important in controlling TFEB activity and plays not only a permissive but also an instructive role. This idea is further supported by our observation that constitutive activation of the growth factor inputs to mTORC1 that occurs in TSC2−/− cells cannot prevent TFEB nuclear accumulation caused by starvation and lysosomal stress. Future work will be required to address how each upstream input to mTOR contributes to TFEB regulation. Nonetheless, compounded with recent evidence showing that amino acid sensing by the v-ATPase/Rag GTPase/mTORC1 may begin in the lysosomal lumen (Zoncu *et al*, 2011a) our findings substantiate the role of TFEB as the end point of a lysosome-sensing and signalling pathway.

Our data shed light into the logic that underlies the control of TFEB localization. In fully fed cells, a fraction of TFEB could always be found on lysosomes, although the majority appeared to freely diffuse in the cytoplasm. The lysosomal localization of TFEB is associated with its ability to physically bind mTORC1, as shown by co-immunoprecipitation assays. Moreover, time-lapse analysis of TFEB–GFP in cells treated with Torin 1 showed that TFEB clustered on lysosomes shortly after the onset of drug treatment, and then progressively appeared in the nucleus (Supplementary Movies S2 and S3). Together, these results suggest the following model of control of TFEB subcellular localization and activity (Figure 7). At any given time, a fraction of TFEB rapidly and transiently binds to the lysosomal surface, where it is phosphorylated by mTORC1 and thus kept in the cytoplasm. Nutrient withdrawal, v-ATPase inhibition, and lysosomal stress inactivate the Rag GTPases, causing loss of mTORC1 from the lysosome and resulting in failure to rephosphorylate TFEB. Unphosphorylated TFEB progressively accumulates in the nucleus, where it activates lysosomal gene expression programs aimed at correcting the defective nutrient and/or pH status of the lysosome. In this model, the lysosome represents a bottleneck where mTORC1 tightly regulates the amount of TFEB that is allowed to reach the nucleus.

mTORC1 may regulate a yet undiscovered TFEB function at the lysosome. This possibility is supported by the observation that blocking mTORC1 activity with Torin 1 resulted in a dramatic accumulation of TFEB not only in the nucleus but also on lysosomes, which was visible as increased binding to mTORC1 in co-IP assays, as well as reduced mobility in FRAP experiments. Future work will address what function, if any, TFEB performs on the lysosomal surface. Interestingly, recent evidence indicating that TFEB regulates multiple aspects of lysosomal dynamics, including the propensity of lysosomes to fuse with the plasma membrane (Medina *et al*, 2011), suggests that the range of biological functions of TFEB still needs to be fully elucidated.

Our data further emphasize the emerging role of the lysosome as a key signalling centre. In particular, a molecular machinery that connects the presence of amino acids in the lysosomal lumen to the activation of mTORC1 indicates a new role for the lysosome in nutrient sensing and cellular growth control (Rabinowitz and White, 2010; Singh and Cuervo, 2011; Zoncu *et al*, 2011a). It also suggests that mTORC1 participates in a lysosomal adaptation mechanism that enables cells to cope with starvation and lysosomal stress conditions (Yu *et al*, 2010). This mechanism responds to a wide range of signals that relay the metabolic state of the cell, as well as the presence of various stress stimuli. For instance, loss of lysosomal proton gradient, caused by either energy depletion or pathological conditions, may suppress mTORC1 activity, either by blocking the proton-coupled transport of nutrients to and from the lysosome, or by directly affecting the v-ATPase (Marshansky, 2007). Similarly, lysosomal membrane permeabilization observed in certain LSDs and neurodegenerative diseases may result in nutrient leakage and suppression of mTORC1 (Dehay *et al*, 2010; Kirkegaard *et al*, 2010).

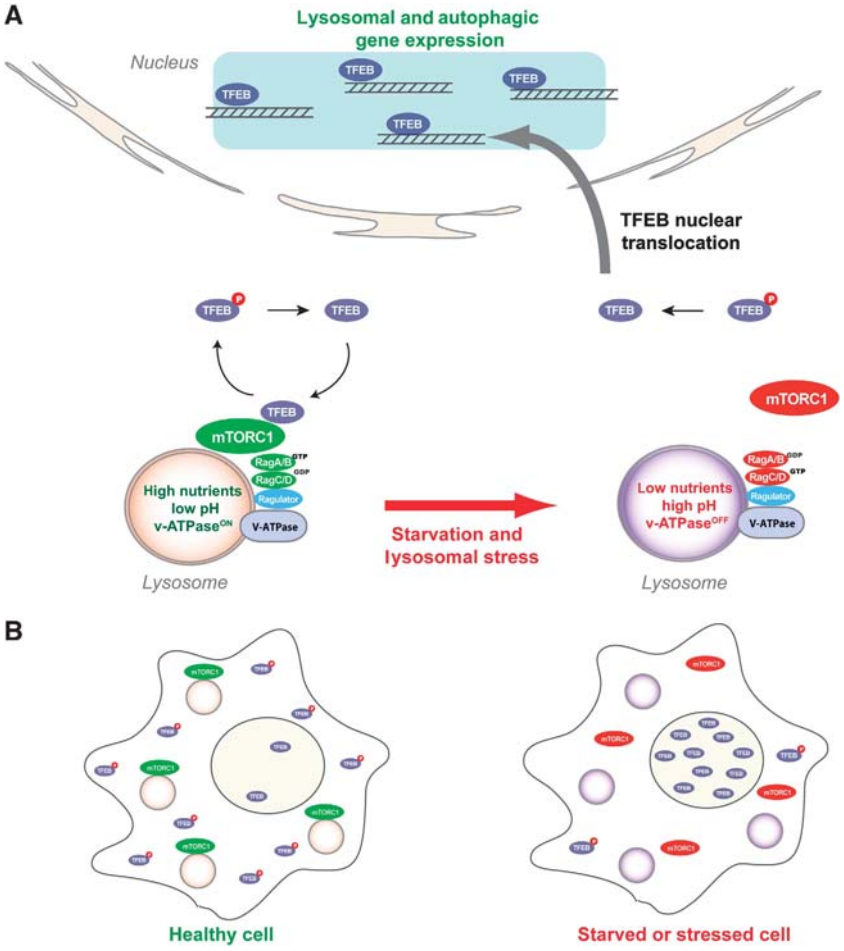

Figure 7 Model of lysosomal sensing and lysosome-to-nucleus signalling by TFEB and mTOR. (**A**) (*Left*) Under full nutrients and in the absence of lysosomal stress, the complex formed by v-ATPase, Ragulator, and Rag GTPases is in the active state and recruits mTORC1 to the lysosomal surface, where mTORC1 becomes activated. At the lysosome, mTORC1 binds and phosphorylates TFEB, which cycles between the cytoplasm and the lysosomal surface. Phosphorylation by mTORC1 maintains TFEB in the cytoplasm and prevents it from translocating to the nucleus. (*Right*) Starvation, v-ATPase inhibition, or lysosomal stress switch the Rags off, leading to mTORC1 detachment from the lysosome and to its inactivation. TFEB can no longer be phosphorylated and translocates to the nucleus, where it activates gene expression programs that boost lysosomal function and autophagy. (**B**) Side-by-side diagrams of a healthy cell and a starved/stressed cell, showing the respective distribution of mTORC1 and TFEB in relationship to lysosomes, cytoplasm, and nucleus.

We found that the transcriptional response of lysosomal and autophagy genes to starvation and mTOR inhibition by Torin 1 was hampered in hepatocytes from mice carrying a liver-specific conditional knockout of TFEB, demonstrating that TFEB is a main mediator of this response. Therefore, TFEB translates a lysosomal signal into a transcriptional program.

This lysosome-to-nucleus signalling mechanism, which operates a feedback regulation of lysosomal function, presents intriguing parallels with the sterol sensing pathway in the endoplasmic reticulum, where cholesterol depletion and ER stress cause the nuclear translocation of the Sterol Responsive Element Binding Protein (SREBP) transcription factor, which then activates gene expression programs that enhance cholesterol synthesis and ER function (Wang *et al*, 1994; Peterson *et al*, 2011). Another example is represented by the mitochondria retrograde signalling pathway, in which mitochondrial dysfunction activates factors such as NFκB, NFAT, and ATF, through altered Ca^{2+} dynamics (Butow and Avadhani, 2004).

Finally, as TFEB overexpression was able to promote substrate clearance and to rescue cellular vacuolization in LSDs (Medina *et al*, 2011), the identification of a lysosome-based, mTOR-mediated, mechanism that regulates TFEB activity offers a new tool to promote cellular clearance in health and disease.

Materials and methods

Cell culture

HeLa and HEK-293T cells were purchased from ATCC and cultured in DMEM supplemented with 10% fetal calf serum, 200 mM L-glutamine, 100 mM sodium pyruvate, penicillin 100 units/ml, streptomycin 100 mg/ml, 5% CO_2 at 37°C. Primary hepatocytes were generated as follow: 2-month-old mice were deeply anaesthetized with Avertin (240 mg/kg) and perfused first with 25 ml of HBSS (Sigma H6648) supplemented with 10 mM HEPES and 0.5 mM EGTA and after with a similar solution containing 100 U/ml of Collagenase (Wako) and 0.05 mg/ml of Trypsin inhibitor (Sigma). Liver was dissociated in a petri dish, cell pellet was washed in HBSS and plated at density of 5×10^5 cells/35 mm dish and cultured in William's medium E supplemented with 10% FBS, 2 mM glutamine, 0.1 μM Insulin, 1 μM Dexamethasone and pen/strep. The next day, cells were treated as described in the text. Sin1−/− and control MEFs were generated as previously described (Jacinto *et al*, 2006) and maintained in DMEM supplemented with 10% FBS, glutamine and pen/strep. TSC2+/+ p53−/− and TSC2−/− p53−/− MEFs,

kindly provided by David Kwiatkowski (Harvard Medical School), were maintained in DMEM supplemented with 10% heat-inactivated FBS, glutamine and pen/strep.

Generation of a Tcfeb*flox mouse line*

We used publicly available embryonic stem (ES) cell clones (http://www.eucomm.org/) in which *Tcfeb* was targeted by homologous recombination at exons 4 and 5. The recombinant ES cell clones were injected into blastocysts, which were used to generate a mouse line carrying the engineered allele. Liver-specific KO was generated crossing the Flox/Flox mice with a transgenic line expressing the CRE under the Albumin promoter (ALB-CRE) obtained from the Jackson laboratory. All procedures involving mice were approved by the Institutional Animal Care and Use Committee of the Baylor College of Medicine.

Plasmids and cell transfection

Cells were transiently transfected with DNA plasmids pRK5-mycPAT1, pRK5-HAGST-Rap2A, pRK5-HAGST-RagB and its Q99L (CA) and T54N (DN) mutants, pRK5-HAGST-RagD and its Q121L (DN) and S77L (CA) mutants; pTFEB-GFP, and pCMV-TFEB-3 × FLAG using lipofectamine2000 or LTX (Invitrogen) according to the protocol from manufacturer. Site-direct mutagenesis was performed according to the manufacturer instructions (Stratagene) verifying the correct mutagenesis by sequencing.

Drugs and cellular treatments

The following drugs were used: Rapamycin (2.5 μM, otherwise indicated) from Sigma; Torin 1 and Torin 2 (250 nM, otherwise indicated) from Biomarine; U0126 (50 μM) from Cell Signaling Technology; Chloroquine (100 μM) from Sigma; Salicylihalamide A (2 μM) was a kind gift from Jeff De Brabander (UT Southwestern).

Immunoblotting and antibodies

The mouse anti-TFEB monoclonal antibody was purchased from My Biosource catalogue No. MBS120432. To generate anti-pS142 specific antibodies, rabbits were immunized with the following peptide coupled to KLH: AGNSAPN{pSer}PMAMLHIC. Following the fourth immunization, rabbits were sacrificed and the serum was collected. Non-phosphospecific antibodies were depleted from the serum by circulation through a column containing the non-phosphorylated antigene. The phosphospecific antibodies were next affinity purified using a column containing the phosphorylated peptide.

Cells were lysed with M-PER buffer (Thermo) containing protease and phosphatase inhibitors (Sigma); nuclear/cytosolic fractions were isolated as previously described (Settembre *et al*, 2011). Proteins were separated by SDS–PAGE (Invitrogen; reduced NuPAGE 4–12% Bis-tris Gel, MES SDS buffer). If needed, the gel was stained using 20 ml Imperial Protein Stain (Thermo Fisher) at room temperature for 1 h and de-stained with water. Immunoblotting analysis was performed by transferring the protein onto a nitrocellulose membrane with an I-Blot (Invitrogen). The membrane was blocked with 5% non-fat milk in TBS-T buffer (TBS containing 0.05% Tween-20) and incubated with primary antibodies anti-FLAG and anti-TUBULIN (Sigma; 1:2000), anti-H3 (Cell Signaling; 1:10 000) at room temperature for 2 h whereas the following antibodies were incubated ON in 5% BSA: anti-TFEB (My Biosource; 1:1000), anti-P TFEB (1:1000) ERK1/2, p-ERK1/2, p-P70S6K, P70S6K (Cell Signaling; 1:1000).

The membrane was washed three times with TBS-T buffer and incubated with alkaline phosphatase-conjugated IgG (Promega; 0.2 mg/ml) at room temperature for 1 h. The membrane was washed three times with TBS buffer and the expressed proteins were visualized by adding 10 ml Western Blue® Stabilized Substrate (Promega).

In-vitro kinase assays

FLAG–S6K1, TFEB–3 × FLAG, and TFEB^{S142A}–3 × FLAG were purified from transiently transfected HEK-293T cells treated with 250 nM Torin 1 for 1 h and lysed in RIPA lysis buffer. The cleared lysates were incubated with FLAG affinity beads (Sigma) for 2 h, washed four times in RIPA containing 500 mM NaCl, and eluted for 1 h at 4°C using a competing FLAG peptide. mTORC1 was purified from HEK-293T cells stably expressing FLAG raptor in 0.3% CHAPS using FLAG affinity beads.

Kinase assays were preincubated for 10 min at 4°C before addition of ATP, and then for 30 min at 30°C in a final volume of 25 μl consisting of kinase buffer (25 mM HEPES, pH 7.4, 50 mM KCl, 10 mM $MgCl_2$) active mTORC1, 250–500 nM substrate, 50 μM ATP, 1 μCi [γ-32P]ATP, and when indicated 250 nM Torin 1. Reactions were stopped by the addition of 6 μl of sample buffer, boiled for 5 min, and analysed by SDS–PAGE followed by autoradiography.

Immunoprecipitation assays

HEK-293T cells that express FLAG-tagged proteins were rinsed once with ice-cold PBS and lysed in ice-cold lysis buffer (150 mM NaCl, 40 mM HEPES (pH 7.4), 2 mM EGTA, 2.5 mM $MgCl_2$, 0.3% CHAPS, and one tablet of EDTA-free protease inhibitors (Roche) per 25 ml). The soluble fractions from cell lysates were isolated by centrifugation at 13 000 r.p.m. for 10 min in a microfuge. For immunoprecipitations, 35 μl of a 50% slurry of anti-FLAG affinity gel (Sigma) was added to each lysate and incubated with rotation for 2–3 h at 4°C. Immunoprecipitates were washed three times with lysis buffer. Immunoprecipitated proteins were denatured by the addition of 35 μl of sample buffer and boiling for 5 min, resolved by 8–16% SDS–PAGE, and analysed by immunoblotting.

Immunofluorescence assays on HEK-293T cells

HEK-293T cells were plated on fibronectin-coated glass coverslips in 35 mm tissue culture dishes, at 300 000 cells/dish. In all, 12–16 h later, cells were transfected with 100 ng of TFEB–3 × FLAG, along with 200 ng Rap2A or Rag GTPase mutants. The next day, cells were subjected to drug treatments or starvation, rinsed with PBS once and fixed for 15 min with 4% paraformaldehyde in PBS at RT. The slides were rinsed twice with PBS and cells were permeabilized with 0.05% Triton X-100 in PBS for 5 min. After rinsing twice with PBS, the slides were incubated with primary antibody in 5% normal donkey serum for 1 h at room temperature, rinsed four times with PBS, and incubated with secondary antibodies produced in donkey (diluted 1:1000 in 5% normal donkey serum) for 45 min at room temperature in the dark, washed four times with PBS. Slides were mounted on glass coverslips using Vectashield (Vector Laboratories) and imaged on a spinning disk confocal system (Perkin-Elmer).

High content nuclear translocation assay

TFEB–GFP cells were seeded in 384-well plates, incubated for 12 h, and treated with 10 different concentrations of ERK inhibitor U0126 (Sigma-Aldrich) and mTOR inhibitors Rapamycin (Sigma-Aldrich), Torin 1 (Biomarin), and Torin 2 (Biomarin), ranging from 2.54 nM to 50 μM. After 3 h at 37°C in RPMI medium, cells were washed, fixed, and stained with DAPI. For the acquisition of the images, 10 pictures per each well of the 384-well plate were taken by using confocal automated microscopy (Opera high content system; Perkin-Elmer). A dedicated script was developed to perform the analysis of TFEB localization on the different images (Acapella software; Perkin-Elmer). The script calculates the ratio value resulting from the average intensity of nuclear TFEB–GFP fluorescence divided by the average of the cytosolic intensity of TFEB–GFP fluorescence. The results were normalized using negative (RPMI medium) and positive (HBSS starvation) control samples in the same plate. The data are represented by the percentage of nuclear translocation at the different concentrations of each compound using Prism software (GraphPad software). The EC50 for each compound was calculated using non-linear regression fitting (Prism software).

Live cell imaging and photobleaching protocol

MEFs were transiently transfected with TFEB–GFP and mRFP–Rab7 by nucleofection (Lonza). Cells were plated on glass bottom 35 mm dishes (MatTek Corp.) at a density of 300 000 cells/dish. The next day, cells were transferred to a physiological imaging buffer (130 mM NaCl, 5 mM KCl, 2.5 mM $CaCl_2$, 2.5 mM $MgCl_2$, 25 mM HEPES) supplemented with 5 mM glucose and imaged on a spinning disk confocal microscope (Andor Technology) with a 488-nm and a 561-nm laser through a × 63 objective. To achieve photobleaching of individual TFEB–GFP-positive lysosomes, areas of interest were drawn around selected spots, and movie acquisition was started. Sixty seconds later, the spots were photobleached with a high power (50 mM) 488 nm pulse (100 μs/pixel illumination) using the Andor FRAPPA unit.

FRAP analysis

The fluorescence recovery of photobleached TFEB-GFP-positive lysosomes was analysed using custom-written plugins in ImageJ (National Institutes of Health). Circular areas of interest were drawn around the spots to be analysed, and the integrated fluorescence within these areas was measured throughout the movie. Fluorescence intensity traces from 5 to 10 spots per condition were normalized to the initial value and time aligned, and their mean and s.d. were calculated using Microsoft Excel. Final plots and curve fitting were made with Prism (GraphPad).

RNA extraction, quantitative PCR, and statistical analysis

Total RNA was extracted from cells using TRIzol (Invitrogen). Reverse transcription was performed using TaqMan reverse transcription reagents (Applied Biosystems). Lysosomal and autophagic gene-specific primers were previously reported (Settembre *et al*, 2011). Fold change values were calculated using the DDCt method. Briefly, GAPDH and Cyclophillin were used as 'normalizer' genes to calculate the DCt value. Next, the DDCt value was calculated between the 'control' group and the 'experimental' group. Lastly, the fold change was calculated using 2(-DDCt). Biological replicates were grouped in the calculation of the fold change values. Unpaired *T*-Test was used to calculate statistical significance. Asterisks in the graph indicate that the *P*-value was <0.05.

mTORC1 phosphosite prediction

In order to identify possible phosphosites that may be targeted by mTORC1, we developed a simple method that quantifies the agreement between regions around serine or threonine sites in TFEB and the mTORC1 phosphorylation motif (Hsu *et al*, 2011). The method calculates the score according to a position-specific score matrix for an amino acid at given distance from the phosphosite of interest. The position starts from -5 and runs to $+4$. The phosphosite is set at position 0. If there is another serine or threonine in this interval, that residue's score is skipped in the sum.

We used MyDomains tool in prosite/expasy.org to sketch the functional domains of TFEB. Domain information was retrieved from UniProt/SwissProt database. Human TFEB and its orthologue sequences were aligned by ClustalW (version 2.0.12), using the default parameters.

Supplementary data

Supplementary data are available at *The EMBO Journal* Online (http://www.embojournal.org).

Acknowledgements

We thank G Diez-Roux for critical reading of the manuscript and S Long for testing TFEB antibodies; I Peluso for help in high content assays; T Kang and C Thoreen for help with mTORC1 kinase assays. We acknowledge the support of the Italian Telethon Foundation (CS, DM, and AB); the Beyond Batten Disease Foundation (CS, DM, FV, SUE, TH, and AB); European Research Council Advanced Investigator grant no. 250154 (AB); the March of Dimes grant # 6-FY11-306 (AB); grants from the National Institutes of Health (R01 CA129105, R01 CA103866 and R37 AI047389) and awards from the American Federation for Aging, Starr Foundation, Koch Institute Frontier Research Program, and the Ellison Medical Foundation to DMS, and fellowships from the Jane Coffin Childs Memorial Fund for Medical Research and the LAM Foundation to RZ DMS in an investigator of Howard Hughes Medical Institute.

Author contributions: CS, RZ, DS, and AB designed the experiments. CS and RZ performed most of the experiments. DM performed high content screening with kinase inhibitors. FV carried out mutagenesis analysis. SE performed bioinformatic analysis. SU and TH provided technical support. MF and GK generated the TFEB phosphoantibody. MV tested TFEB antibodies. VF generated SIN1−/− MEFs. CS, RZ, and AB wrote the paper.

Conflict of interest

The authors declare that they have no conflict of interest.

References

Ballabio A, Gieselmann V (2009) Lysosomal disorders: from storage to cellular damage. *Biochim Biophys Acta* **1793:** 684–696

Butow RA, Avadhani NG (2004) Mitochondrial signaling: the retrograde response. *Mol Cell* **14:** 1–15

Dehay B, Bove J, Rodriguez-Muela N, Perier C, Recasens A, Boya P, Vila M (2010) Pathogenic lysosomal depletion in Parkinson's disease. *J Neurosci* **30:** 12535–12544

Dephoure N, Zhou C, Villen J, Beausoleil SA, Bakalarski CE, Elledge SJ, Gygi SP (2008) A quantitative atlas of mitotic phosphorylation. *Proc Natl Acad Sci USA* **105:** 10762–10767

Feldman ME, Apsel B, Uotila A, Loewith R, Knight ZA, Ruggero D, Shokat KM (2009) Active-site inhibitors of mTOR target rapamycin-resistant outputs of mTORC1 and mTORC2. *PLoS Biol* **7:** e38

Frias MA, Thoreen CC, Jaffe JD, Schroder W, Sculley T, Carr SA, Sabatini DM (2006) mSin1 is necessary for Akt/PKB phosphorylation, and its isoforms define three distinct mTORC2s. *Curr Biol* **16:** 1865–1870

Garcia-Martinez JM, Moran J, Clarke RG, Gray A, Cosulich SC, Chresta CM, Alessi DR (2009) Ku-0063794 is a specific inhibitor of the mammalian target of rapamycin (mTOR). *Biochem J* **421:** 29–42

Hsu PP, Kang SA, Rameseder J, Zhang Y, Ottina KA, Lim D, Peterson TR, Choi Y, Gray NS, Yaffe MB, Marto JA, Sabatini DM (2011) The mTOR-regulated phosphoproteome reveals a mechanism of mTORC1-mediated inhibition of growth factor signaling. *Science* **332:** 1317–1322

Jacinto E, Facchinetti V, Liu D, Soto N, Wei S, Jung SY, Huang Q, Qin J, Su B (2006) SIN1/MIP1 maintains rictor-mTOR complex integrity and regulates Akt phosphorylation and substrate specificity. *Cell* **127:** 125–137

Kim E, Goraksha-Hicks P, Li L, Neufeld TP, Guan KL (2008) Regulation of TORC1 by Rag GTPases in nutrient response. *Nat Cell Biol* **10:** 935–945

Kirkegaard T, Roth AG, Petersen NH, Mahalka AK, Olsen OD, Moilanen I, Zylicz A, Knudsen J, Sandhoff K, Arenz C, Kinnunen PK, Nylandsted J, Jaattela M (2010) Hsp70 stabilizes lysosomes and reverts Niemann-Pick disease-associated lysosomal pathology. *Nature* **463:** 549–553

Luzio JP, Pryor PR, Bright NA (2007) Lysosomes: fusion and function. *Nat Rev Mol Cell Biol* **8:** 622–632

Marshansky V (2007) The V-ATPase a2-subunit as a putative endosomal pH-sensor. *Biochem Soc Trans* **35:** 1092–1099

Medina DL, Fraldi A, Bouche V, Annunziata F, Mansueto G, Spampanato C, Puri C, Pignata A, Martina JA, Sardiello M, Palmieri M, Polishchuk R, Puertollano R, Ballabio A (2011) Transcriptional activation of lysosomal exocytosis promotes cellular clearance. *Dev Cell* **21:** 421–430

Palmieri M, Impey S, Kang H, di Ronza A, Pelz C, Sardiello M, Ballabio A (2011) Characterization of the CLEAR network reveals an integrated control of cellular clearance pathways. *Hum Mol Genet* **20:** 3852–3866

Pena-Llopis S, Vega-Rubin-de-Celis S, Schwartz JC, Wolff NC, Tran TA, Zou L, Xie XJ, Corey DR, Brugarolas J (2011) Regulation of TFEB and V-ATPases by mTORC1. *EMBO J* **30:** 3242–3258

Peterson TR, Sengupta SS, Harris TE, Carmack AE, Kang SA, Balderas E, Guertin DA, Madden KL, Carpenter AE, Finck BN, Sabatini DM (2011) mTOR complex 1 regulates lipin 1 localization to control the SREBP pathway. *Cell* **146:** 408–420

Rabinowitz JD, White E (2010) Autophagy and metabolism. *Science* **330:** 1344–1348

Saftig P, Klumperman J (2009) Lysosome biogenesis and lysosomal membrane proteins: trafficking meets function. *Nat Rev Mol Cell Biol* **10:** 623–635

Sagne C, Agulhon C, Ravassard P, Darmon M, Hamon M, El Mestikawy S, Gasnier B, Giros B (2001) Identification and characterization of a lysosomal transporter for small neutral amino acids. *Proc Natl Acad Sci USA* **98:** 7206–7211

Sancak Y, Bar-Peled L, Zoncu R, Markhard AL, Nada S, Sabatini DM (2010) Ragulator-Rag complex targets mTORC1 to the lysosomal surface and is necessary for its activation by amino acids. *Cell* **141:** 290–303

Sancak Y, Peterson TR, Shaul YD, Lindquist RA, Thoreen CC, Bar-Peled L, Sabatini DM (2008) The Rag GTPases bind raptor and mediate amino acid signaling to mTORC1. *Science* **320:** 1496–1501

Sardiello M, Palmieri M, di Ronza A, Medina DL, Valenza M, Gennarino VA, Di Malta C, Donaudy F, Embrione V, Polishchuk RS, Banfi S, Parenti G, Cattaneo E, Ballabio A (2009) A gene network regulating lysosomal biogenesis and function. *Science* **325:** 473–477

Settembre C, Ballabio A (2011) TFEB regulates autophagy: an integrated coordination of cellular degradation and recycling processes. *Autophagy* **7:** 1379–1381

Settembre C, Di Malta C, Polito VA, Garcia Arencibia M, Vetrini F, Erdin S, Erdin SU, Huynh T, Medina D, Colella P, Sardiello M, Rubinsztein DC, Ballabio A (2011) TFEB links autophagy to lysosomal biogenesis. *Science* **332:** 1429–1433

Singh R, Cuervo AM (2011) Autophagy in the cellular energetic balance. *Cell Metab* **13:** 495–504

Thoreen CC, Kang SA, Chang JW, Liu Q, Zhang J, Gao Y, Reichling LJ, Sim T, Sabatini DM, Gray NS (2009) An ATP-competitive mammalian target of rapamycin inhibitor reveals rapamycin-resistant functions of mTORC1. *J Biol Chem* **284:** 8023–8032

Wang X, Sato R, Brown MS, Hua X, Goldstein JL (1994) SREBP-1, a membrane-bound transcription factor released by sterol-regulated proteolysis. *Cell* **77:** 53–62

Xie XS, Padron D, Liao X, Wang J, Roth MG, De Brabander JK (2004) Salicylihalamide A inhibits the V0 sector of the V-ATPase through a mechanism distinct from bafilomycin A1. *J Biol Chem* **279:** 19755–19763

Yang Q, Inoki K, Ikenoue T, Guan KL (2006) Identification of Sin1 as an essential TORC2 component required for complex formation and kinase activity. *Genes Dev* **20:** 2820–2832

Yu L, McPhee CK, Zheng L, Mardones GA, Rong Y, Peng J, Mi N, Zhao Y, Liu Z, Wan F, Hailey DW, Oorschot V, Klumperman J, Baehrecke EH, Lenardo MJ (2010) Termination of autophagy and reformation of lysosomes regulated by mTOR. *Nature* **465:** 942–946

Yu Y, Yoon SO, Poulogiannis G, Yang Q, Ma XM, Villen J, Kubica N, Hoffman GR, Cantley LC, Gygi SP, Blenis J (2011) Phosphoproteomic analysis identifies Grb10 as an mTORC1 substrate that negatively regulates insulin signaling. *Science* **332:** 1322–1326

Zoncu R, Bar-Peled L, Efeyan A, Wang S, Sancak Y, Sabatini DM (2011a) mTORC1 senses lysosomal amino acids through an inside-out mechanism that requires the vacuolar H-ATPase. *Science* **334:** 678–683

Zoncu R, Efeyan A, Sabatini DM (2011b) mTOR: from growth signal integration to cancer, diabetes and ageing. *Nat Rev Mol Cell Biol* **12:** 21–35

